X-ray Crystal Structures of *Candida albicans* Dihydrofolate Reductase: High Resolution Ternary Complexes in Which the Dihydronicotinamide Moiety of NADPH Is Displaced by an Inhibitor

Marc Whitlow,[†,§] Andrew J. Howard,[†,∥] David Stewart,[†,○] Karl D. Hardman,[†,#] Joseph H. Chan,[‡] David P. Baccanari,[‡] Robert L. Tansik,[‡] Jean S. Hong,[‡,⊥] and Lee F. Kuyper*[,‡]

GlaxoSmithKline, Inc., Five Moore Drive, Research Triangle Park, North Carolina 27709

X-ray crystallographic analysis of 5-(4′-substituted phenyl)sulfanyl-2,4-diaminoquinazoline inhibitors in ternary complex with *Candida albicans* dihydrofolate reductase (DHFR) and NADPH revealed two distinct modes of binding. The two compounds with small 4′-substituents (H and CH_3) were found to bind with the phenyl group oriented in the plane of the quinazoline ring system and positioned adjacent to the C-helix. In contrast, the more selective inhibitors with larger 4′-substituents (*tert*-butyl and *N*-morpholino) were bound to the enzyme with the phenyl group perpendicular to the quinazoline ring and positioned in the region of the active site that typically binds the dihydronicotinamide moiety of NADPH. The cofactor appeared bound to DHFR but with the disordered dihydronicotinamide swung away from the protein surface and into solution. This unusual inhibitor binding mode may play an important role in the high DHFR selectivity of these compounds and also may provide new ideas for inhibitor design.

Introduction

The frequency of invasive fungal infections has increased markedly in recent years.[1] Life-threatening disease caused by opportunistic fungal organisms such as *Candida albicans*, *Cryptococcus neoformans*, and *Aspergillus fumigatus* is now relatively common among patients whose immune systems are compromised by cancer chemotherapy, organ transplantation procedures, aggressive surgical intervention, or AIDS.[2−5] Candida species are particularly prevalent and have become nearly as common a cause of hospital-acquired sepsis as the familiar bacterial pathogens.[6]

In contrast to the large number of agents available for fighting bacterial diseases, drugs that are effective in the treatment of systemic fungal infections are few.[7,8] Novel, safe, and effective antifungal agents are clearly needed. As part of a program focused on developing new medicines for antifungal therapy, we have investigated the use of inhibitors of *C. albicans* dihydrofolate reductase (DHFR). DHFR is a well-established target for drug action and serves as the molecular receptor for the antibacterial agent trimethoprim (**1**). The clinical utility of **1** stems from its highly selective inhibition of bacterial DHFR: the affinity of **1** for *Escherichia coli* DHFR is

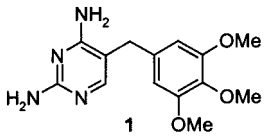

1

12,000-fold greater than that for the corresponding human enzyme. Our intent was to develop compounds with analogous selectivity for fungal DHFR.

To aid our effort to devise selective inhibitors of fungal DHFR, we have determined the three-dimensional molecular structure of *C. albicans* DHFR using X-ray crystallography. Our studies of the *C. albicans* DHFR−NADPH binary complex and a ternary complex containing the nonselective inhibitor **2** have been reported.[9] In this paper, we report structures of four ternary complexes of the fungal enzyme in which 5-phenylthioquinazoline inhibitors,[10] compounds **3**−**6**, were bound to the DHFR/NADPH complex. Two types of binding

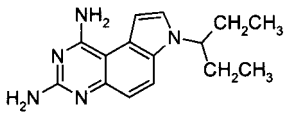

2

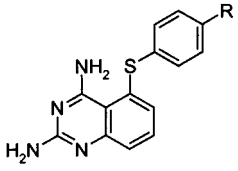

3: R = H
4: R = CH_3
5: R = $C(CH_3)_3$
6: R = N O

mode were observed. Inhibitors **3** and **4** were found to bind as expected, with the 5-phenylthio group oriented against the C-helix. However, compounds **5** and **6** were found to bind to *C. albicans* DHFR in a manner unprecedented in previous studies of DHFR-inhibitor complexes. The 5-phenylthio groups of these latter two inhibitors were positioned in the region of the active site

* To whom reprint requests should be addressed: GlaxoSmithKline, Inc., 5 Moore Drive, Research Triangle Park, NC 27709. Telephone: (919)-483-2114. Fax: (919)-483-6053. E-mail: lfk30687@gsk.com.

† Work was performed at Genex Corporation, Gathersburg, MD.

‡ Work was performed at Burroughs Wellcome Co., Research Triangle Park, NC.

§ Present address: Department of Biophysics, Berlex Biosciences, 15049 San Pablo Ave., Richmond, CA 94804.

∥ Present address: IMCA Collaborative Access Team, Department of Biological, Chemical, and Physical Sciences, Illinois Institute of Technology, 3101 South Dearborn, Chicago, IL 60616.

○ Deceased.

Present address: Dupont Pharmaceuticals Co., Experimental Station E353/148H, Wilmington, DE 19880-0353.

⊥ Present address: Scynexis Chemistry and Automation Inc., Research Triangle Park, NC 27709.

10.1021/jm0101444 CCC: $20.00
Published on Web 08/04/2001

Table 1. DHFR Inhibition Data for Compounds **2**−**6**

compd	DHFR IC_{50} (μM) *C. albicans*	DHFR IC_{50} (μM) human	selectivity index (human/*C. albicans* DHFR IC_{50})
2	0.0040[a]	0.0066[a]	1.7
3	0.034	0.62	18
4	0.023	0.94	41
5	0.008	2.0	250
6	0.13	70	540

[a] IC_{50} value calculated from measured K_i.

cleft that is typically occupied by the dihydronicotinamide unit of NADPH. Although electron density for the adenosine and diphosphate moieties of cofactor was observed in the expected region of the protein surface, density for the dihydronicotinamide portion of NADPH was not observed, suggesting that it was extended into solvent and was disordered. Compounds **5** and **6** are the most selective inhibitors of fungal DHFR reported to date, implicating the competition with NADPH as a potentially important factor contributing to the enzyme selectivity.

Results and Discussion

DHFR Activity and Selectivity of Compounds 3−6. The 5-arylthioquinazolines, represented by compounds **3**−**6**, are potent and selective inhibitors of *C. albicans* DHFR.[10] As shown in Table 1, the DHFR activity and selectivity is significantly influenced by the para substituents on the phenyl ring. The parent compound **3** (R = H) is a potent inhibitor of the fungal enzyme and is 18-fold less active against human DHFR. The activity of the *p*-methyl derivative **4** is slightly higher than that of the parent compound against the *C. albicans* enzyme and correspondingly lower against human DHFR, yielding a selectivity index for compound **4** about 2-fold higher than that of compound **3**. The bulkier substituents of compounds **5** and **6** impart a significant increase in DHFR selectivity. The *tert*-butyl substituted analogue **5** is the most potent inhibitor of *C. albicans* DHFR in the series (IC_{50} = 8 nM) and exhibits a selectivity index of 250. Although the morpholino derivative (**6**) is the weakest inhibitor of the set, it is also the most selective, inhibiting the fungal DHFR 540-fold more effectively than human enzyme.

Common Features of All Four Inhibitor/*C. albicans* DHFR Crystal Structures. X-ray crystallographic analysis of *C. albicans* DHFR has been reported previously.[9] As in the previously reported structures, the structures reported here exhibit an asymmetric unit composed of two independent complexes. The active sites of the two complexes are essentially identical, although complex 1 appears to be distorted by intermolecular crystal contacts in a region distant from the active site of the protein involving residues 1−5, 45−47, and 94−105. For the sake of brevity, discussions here will focus on complex 2, although conclusions regarding inhibitor−protein interactions can be drawn similarly from complex 1. The previously reported structures of the *C. albicans* enzyme in binary complex with NADPH and in ternary complex with the nonselective inhibitor **2** display a protein fold that is characteristic of DHFR from many other species.[9] A nine-stranded β-sheet forms the core of the protein and is flanked on either side by α-helices. The same protein fold was observed for the enzyme complexes with compounds **3**−**6**. The active site is located between helices B and C. Glu-32, which is near the center of the B-helix, provides a key interaction with the 2,4-diaminopyrimidine class of inhibitor.

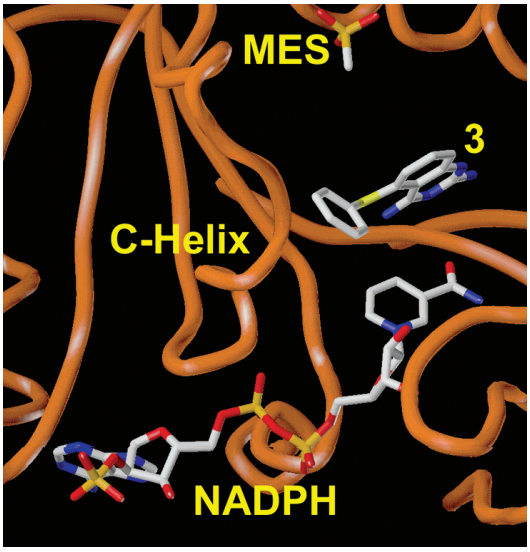

Figure 1. Structure of compound **3** bound to *C. albicans* DHFR/NADPH. Protein is represented as a red-orange tube, and ligands are color-coded by atom type as follows: C, white; N, blue; O, red; S, yellow; P, tan.

The 2,4-diaminoquinazoline rings of compounds **3**−**6** were found to interact with *C. albicans* DHFR in a manner similar to that observed for compound **2**.[9] As found for other related inhibitors of DHFR,[11−15] the diaminopyrimidine ring was linked to protein by five hydrogen bonds. The 4-amino group donated hydrogen bonds to the backbone carbonyl groups of Ile-9 and Ile-112. One hydrogen atom of the 2-amino group was hydrogen bonded to a conserved water molecule, which in turn donated hydrogen bonds to the side chain of Thr-133 and the backbone carbonyl of Leu-131. The other hydrogen of the 2-amino group, accompanied by the presumed hydrogen at the protonated N1 atom of the pyrimidine ring,[16,17] interacted with the carboxylate functionality of Glu-32.

Differences among the four structures were found primarily in interactions involving the phenylthio moiety and are discussed below.

Crystal Structures of *C. albicans* DHFR in Complex with Compounds 3 and 4. Compounds **3** and **4** differ in chemical structure by a single methyl group at the para position of the phenylthio group, and the corresponding complexes with *C. albicans* DHFR were similar. The structure of the DHFR complex with compound **3** is shown in Figure 1. The phenylthio moiety of each inhibitor was oriented adjacent to the C-helix on the left side of the binding cleft near Met-54, Thr-58, Ser-61, Ile-62, Leu-69, and Ile-112. The conformation-defining torsion angles T_1 (C4a−C5−S−C1′) and T_2 (C5−S−C1′−C2′) were 165° and 108° for compound **3** and 161° and 112° for compound **4**, respectively. The phenyl group of compound **3** was within 4 Å of the side chains of Thr-58, Ser-61, and Ile-62 and the C5 atom of the nicotinamide unit of NADPH. Similar contacts were found for the phenyl group of compound **4**, and the *p*-methyl group also had close contact with the amide unit that joins Ser-61 and Ile-62.

NADPH was bound in typical fashion in both complexes. The nicotinamide ring was positioned below the diaminoquinazoline ring system of the inhibitors and was linked to the backbone NH and CO groups of Ala-11 through two hydrogen bonds via its pendant amide group.

The complex containing compound **4** also contained a molecule of the buffer 2-(*N*-morpholino)ethanesulfonate (MES) with its sulfonate group involved in an ionic bond to Arg-70, the expected site of interaction for the α-carboxyl group of substrate dihydrofolate.[18] The morpholinoethyl unit was positioned downward into the active site, and its ether oxygen was in contact with the arylthio group of the inhibitor. A disordered MES molecule is presumably present in the complex with compound **3**, but electron density was observed only in the region of the sulfonate moiety. The effect of MES on the observed binding mode of compounds **3** and **4** is not known. A corresponding MES molecule was also present in the DHFR complexes with compounds **5** and **6**, as discussed below.

As discussed by Whitlow et al.,[9] the *C. albicans* DHFR structure exhibits an active site cleft that is significantly wider than that observed for human DHFR, and the difference in cleft width might provide a basis for inhibitor selectivity. The *C. albicans* versus human DHFR selectivity and the observed binding of compounds **3** and **4** were consistent with that notion. The two inhibitors appear to take good advantage of the relatively wide cleft of the fungal enzyme by snugly wedging between helices B and C. Compounds **3** and **4** appear to require some widening of the *C. albicans* DHFR active site as indicated by the comparison of active site geometries of those two complexes with that of the holoenzyme or the complex with the nonselective compound **2**. For example, the cleft of *C. albicans* DHFR in complex with compound **4** is 0.7−1.1 Å wider than that of the corresponding complex with compound **2**. The geometry differences for the enzyme in those two complexes is illustrated by the following α-carbon distance differences (distance in compound **2** complex minus distance in compound **4** complex): Glu-32−Leu-62 (0.7 Å), Glu-32−Ser-61 (0.8 Å), Met-25−Ile-62 (1.0 Å), Lys-24−Ser-61 (1.1 Å), and Gly-23−Glu-60 (0.8 Å). On the basis of the observed geometry of human DHFR,[19] that enzyme would require even greater widening to accommodate compounds **3** and **4**. The expected energetic cost of such widening was consistent with the observed *C. albicans* vs human DHFR selectivity of compounds **3** and **4**.

Crystal Structures of *C. albicans* DHFR in Complex with Compounds 5 and 6. The bound conformations of compounds **5** and **6** were significantly different than those of **3** and **4**. The more selective inhibitors **5** and **6** were found to bind in conformations in which the S-to-phenyl bond of the phenylthio group was oriented perpendicularly to the quinazoline ring system, projecting the group into the region of the active site that is normally occupied by the nicotinamide moiety of NADPH, as illustrated for compound **5** in Figure 2. For compounds **5** and **6**, the torsion angle T_1 was 89° and 92°, respectively, compared to the average value of 163° for compounds **3** and **4**. T_2 values for compounds **5** and **6** were 160° and 170°, respectively. The conformational

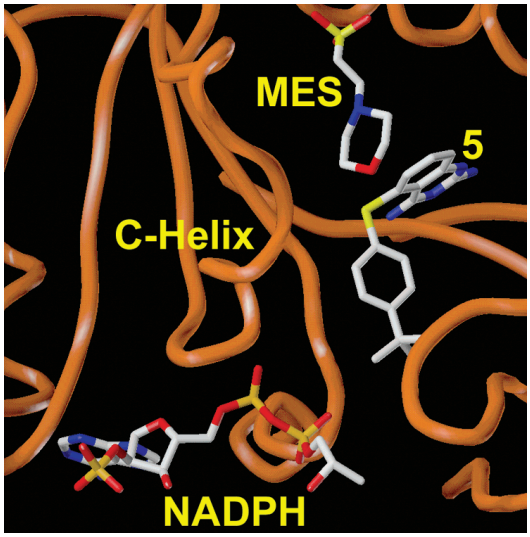

Figure 2. Structure of compound **5** bound to *C. albicans* DHFR/NADPH. Protein structure is represented as described in Figure 1, and ligands are color-coded by atom type as described in Figure 1.

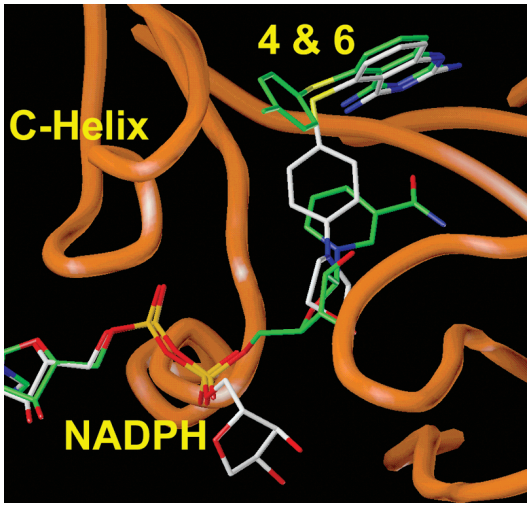

Figure 3. Comparison of compounds **4** and **6** bound to *C. albicans* DHFR/NADPH. Protein structure is from the compound **6** complex and is represented as described in Figure 1. Ligands are color-coded by atom type as described in Figure 1 with the exception of carbon for the ligands of the complex with compound **4**, which are colored green. The MES molecules are omitted for clarity.

difference between compounds **4** and **6** is illustrated in Figure 3.

The binding of compounds **5** and **6** appeared to displace the dihydronicotinamide moiety of NADPH from its typical location within the active site and into solvent. Electron density was observed for the adenosine and phospho bridge portions of the cofactor, but density at the dihydronicotinamide end of the molecule was limited to just a few atoms of the ribose ring, consistent with disorder for that section of NADPH.

Molecular modeling of compounds **5** and **6** in a binding conformation analogous to that observed for compounds **3** and **4** suggested that the *tert*-butyl and morpholino substituents of compounds **5** and **6**, respectively, would encounter unfavorable steric interactions with residues at the carboxy-terminus of the C-helix, such as Ser-61 and Ile-62. Presumably the energetic cost

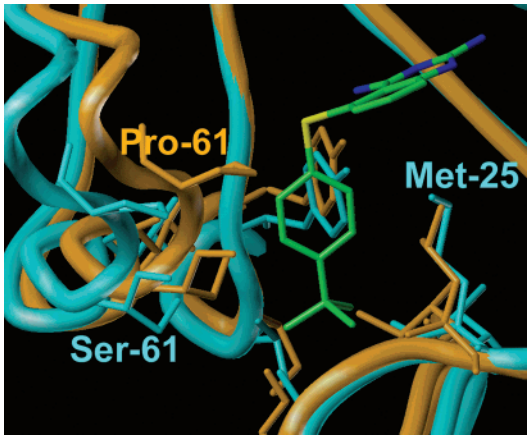

Figure 4. Binding site for the *p-tert*-butylphenylthio moiety of compound **5** in *C. albicans* DHFR compared to the corresponding region of human DHFR (PDB code: 1boz). Protein backbone is represented by a tube: *C. albicans*, cyan; human, orange. Atoms of selected amino acid residues are shown as capped sticks. Compound **5** is color-coded by atom type: C, green; N, blue; S, yellow. Superposition of the two proteins was based on α-carbon atoms of the central β-sheet.

involved in protein conformational changes to alleviate that steric clash was higher than the alternative displacement of the dihydronicotinamide group of NADPH.

Although inhibitor occupation of the nicotinamide binding site has not been reported previously, conformational heterogeneity for NADPH and $NADP^+$ in DHFR complexes that is concordant with the structures presented here has been observed. For example, results from fluorescence decay measurements for NADPH bound to *Escherichia coli* DHFR were attributed to two conformational states of enzyme-bound cofactor: one in which the dihydronicotinamide moiety is solvent-exposed and a second species in which the dihydronicotinamide is sequestered from solvent.[20] Similar conclusions were drawn for $NADP^+$ from NMR studies of ternary complexes with *Lactobacillus casei* DHFR and a series of inhibitors.[21] The ternary complexes showed evidence of two interconverting conformations that differed in the position of the nicotinamide moiety of the enzyme-bound cofactor, one within the enzyme active site and one swung away from the enzyme surface into solution. Furthermore, crystallographic analysis of an *E. coli* DHFR/NADP+ complex showed that the nicotinamide group of bound cofactor was disordered and appeared to extend away from the protein and into solvent.[22]

The high level of DHFR selectivity observed for compounds **5** and **6** may be in part related to the apparent competition for DHFR binding with the dihydronicotinamide moiety of NADPH. The cofactor shows about 10-fold higher affinity for human DHFR than the corresponding fungal enzyme as evidenced by K_m values (NADPH K_m: human DHFR, 0.26 μM;[23] *C. albicans* DHFR, 3.3 μM[24]). If the difference in NADPH affinity between human and fungal enzyme was due to differential interactions involving the dihydronicotinamide group, then inhibitor competition with that group should result in greater inhibitor affinity for the enzyme with the higher NADPH K_m. The binding site for the dihydronicotinamide, and presumably the arylthio group of compounds **5** and **6**, in human DHFR[25] was significantly different than that of the fungal enzyme (see Figure 4). In particular, the difference in position of the C-helix in the two DHFR species led to dissimilar environments in that part of the active site. As shown in Figure 4, the positions of side chains from Thr-56, Ser-59, and Pro-61 in the human protein relative to those of *C. albicans* DHFR create a smaller cavity for binding dihydronicotinamide or inihibitor.

Table 2. Summary of Crystallographic Refinement

	3	4	5	6
PDB code	1IA1	1IA2	1IA3	1IA4
space group	$P2_1$	$P2_1$	$P2_1$	$P2_1$
unit cell dimensions	$a = 76.91$	$a = 76.91$	$a = 76.91$	$a = 77.05$
	$b = 67.28$	$b = 67.28$	$b = 67.28$	$b = 67.09$
	$c = 38.49$	$c = 38.49$	$c = 38.49$	$c = 38.54$
	$\beta = 93.07$	$\beta = 93.07$	$\beta = 93.07$	$\beta = 93.43$
resolution (Å)	1.70	1.82	1.78	1.85
no. reflections				
measured	34713	35760	36058	34740
used ($F > 2s$)	31488	31067	32308	26626
R factor[a]	0.156	0.160	0.160	0.159
distances (Å)				
bonds(1−2)	0.021	0.021	0.021	0.021
angles (1−3)	0.034	0.032	0.034	0.035
intraplanar (1−4)	0.040	0.038	0.040	0.041
planar groups (Å)	0.021	0.020	0.021	0.020
chiral centers (Å^3)	0.276	0.247	0.243	0.258
nonbonding contacts (Å)				
single torsion	0.166	0.166	0.167	0.170
multiple torsion	0.154	0.148	0.148	0.150
possible H-bonds	0.127	0.133	0.136	0.150
torsion angles (deg)				
planar (w)	4.0	3.6	3.8	3.9
staggered	16.1	14.6	14.9	14.9
orthonormal	31.4	30.6	32.6	29.9

[a] R factor $= \Sigma|F_o - F_c|/\Sigma F_o$.

Conclusions

Compounds **5** and **6** were found to bind to *C. albicans* DHFR in an unusual mode, displacing the dihydronicotinamide portion of NADPH from its normal position within the enzyme active site. Inhibitor binding in the dihydronicotinamide binding site of DHFR has not been reported previously. The observation that highly selective inhibitors of fungal DHFR utilize the dihydronicotinamide site suggests a potential role for the site in achieving therapeutically useful DHFR selectivity and offers a new approach to the design of DHFR inhibitors.

Experimental Section

The cloning, expression, purification, and crystallization of *C. albicans* DHFR employed procedures that have been described previously.[9] The preparation and biological activities of compounds **3**−**6** have been reported by Chan et al.[10]

X-ray diffraction data were collected using a Siemens (formerly Xentronics) electronic area detector mounted on a Supper oscillation camera on an Elliot GX-21 rotating Cu anode, operating at 70 mA and 40 kV with a 0.3 × 3.0 mm focal spot and a 0.3 mm collimator. Monochromatization was provided by a Huber graphite monochromator. All data collection was performed at well-controlled room temperature (16−20 °C). During data collection, the area detector chamber was mounted 10 cm from the crystal. The carriage angle (the angle between the normal to the detector face and the direct beam) was varied from 0° to 30°, enabling the detector to intercept data from 8 to 1.70 Å, depending upon its position. Diffraction data collected by the area detector are recorded as a series of discrete frames or electronic images, each comprising a 0.20° or 0.25° oscillation counted for between 30 and 110 s, depending upon the carriage angle. Usually 400 to 480 data

frames, corresponding to 100° of crystal rotation about a vertical axis, were collected. The crystals were very stable in the X-ray beam allowing collection of an extensively replicated data set to 1.70 Å from a single crystal. During the course of data collection, several crystal orientations were recorded. The crystals were repositioned in the X-ray beam by adjustment of a goniostat ϕ motor set 45° from vertical. The *XENGEN* software package was used for data reduction.[26]

The refinement of each ternary structure was started from the highest resolution structure available at the time. The binary structure described in the previous paper[9] was used for the ternary complex with compound **2**; all the others used the 1.6 Å structure ternary inhibited complex[9] as starting coordinates. Each structure was refined using the program PROFFT, which employs a least squares procedures[27] modified by Finzel[28] to incorporate the fast Fourier algorithms of Ten Eyck and Agarwal.[29,30] Refinement was performed interspersed with model-building sessions on the graphics equipment. Temperature factors were not restrained in the final cycles of refinement. The refinement results are summarized in Table 2. Atomic coordinates of the four ternary DHFR complexes containing compounds **3**−**6** have been deposited with the Protein Data Bank, PDB entries 1IA1, 1IA2, 1IA3, and 1IA4, respectively.

References

(1) De Pauw, B. E.; Meunier, F. The challenge of invasive fungal infection. *Chemotherapy* (*Basel*) **1999**, *45*, 1−14.

(2) Rex, J. H.; Walsh, T. J.; Anaissie, E. J. Fungal infections in iatrogenically compromised hosts. *Adv. Intern. Med.* **1998**, *43*, 321−371.

(3) Fichtenbaum, C. J.; Powderly, W. G. Refractory mucosal Candidiasis in patients with human immunodeficiency virus infection. *Clin. Infect. Dis.* **1998**, *26*, 556−565.

(4) Graybill, J. R. The future of antifungal therapy. *Clin. Infect. Dis.* **1996**, *22*, S166−178.

(5) Sternberg, S. The emerging fungal threat. *Science* **1994**, *266*, 1632−1634.

(6) Edwards, J. E. Invasive Candida infections. Evolution of a fungal pathogen. *N. Engl. J. Med.* **1991**, *324*, 1060−1062.

(7) Barnes, R. A. Approaches to antifungal therapy in the intensive care unit. *Curr. Opin. Infect. Dis.* **2000**, *13*, 609−614.

(8) Balkovec, J. M. Nonazole antifungal agents. *Ann. Rep. Med. Chem.* **1998**, *33*, 173−182.

(9) Whitlow, M.; Howard, A. J.; Stewart, D.; Hardman, K. D.; Kuyper, L. F. et al. X-ray crystallographic studies of *Candida albicans* dihydrofolate reductase: High-resolution structures of the holoenzyme and an inhibited ternary complex. *J. Biol. Chem.* **1997**, *272*, 30289−30298.

(10) Chan, J. H.; Hong, J. S.; Kuyper, L. F.; Baccanari, D. P.; Joyner, S. S. et al. Selective inhibitors of *Candida albicans* dihydrofolate reductase: Activity and selectivity of 5-(arylthio)-2,4-diaminoquinazolines. *J. Med. Chem.* **1995**, *38*, 3608−3616.

(11) Baker, D. J.; Beddell, C. R.; Champness, J. N.; Goodford, P. J.; Norrington, F. E. A. et al. The binding of trimethoprim to bacterial dihydrofolate reductase. *FEBS Lett.* **1981**, *126*, 49−52.

(12) Bolin, J. T.; Filman, D. J.; Matthews, D. A.; Hamlin, R. C.; Kraut, J. Crystal structures of *Escherichia coli* and *Lactobacillus casei* dihydrofolate reductase refined at 1.7A resolution. I. General features and binding of methotrexate. *J. Biol. Chem.* **1982**, *257*, 13650−13662.

(13) Champness, J. N.; Stammers, D. K.; Beddell, C. R. Crystallographic investigation of the cooperative interaction between trimethoprim, reduced cofactor and dihydrofolate reductase. *FEBS Lett.* **1986**, *199*, 61−67.

(14) Filman, D. J.; Bolin, J. T.; Matthews, D. A.; Kraut, J. Crystal structures of *Escherichia coli* and *Lactobacillus casei* dihydrofolate reductase refined at 1.7A resolution. II. Environment of bound NADPH and implications for catalysis. *J. Biol. Chem.* **1982**, *257*, 13663−13672.

(15) Kuyper, L. F.; Roth, B.; Baccanari, D. P.; Ferone, R.; Beddell, C. R. et al. Receptor-based design of dihydrofolate reductase inhibitors: Comparison of crystallographically determined enzyme binding with enzyme affinity in a series of carboxy-substituted trimethoprim analogues. *J. Med. Chem.* **1985**, *28*, 303−311.

(16) Bevan, A. W.; Roberts, G. C. K.; Feeney, J.; Kuyper, L. F. 1H and 15N NMR studies of protonation and hydrogen-bonding in the binding of trimethoprim to dihydrofolate reductase. *Eur. Biophys. J.* **1985**, *11*, 211−218.

(17) Cocco, L.; Roth, B.; Temple, C., Jr.; Montgomery, J. A.; London, R. E. et al. Protonated state of methotrexate, trimethoprim, and pyrimethamine bound to dihydrofolate reductase. *Arch. Biochem. Biophys.* **1983**, *226*, 567−577.

(18) Kraut, J.; Matthews, D. A. Dihydrofolate reductase. *Biological Macromolecules and Assemblies*; Wiley: New York, 1987; pp 1−71.

(19) Davies, J. F.; Delcamp, T. J.; Prendergast, N. J.; Ashford, V. A.; Freisheim, J. H. et al. Crystal structures of recombinant human dihydrofolate reductase complexed with folate and 5-deazafolate. *Biochemistry* **1990**, *29*, 9467−9479.

(20) Farnum, M. F.; Magde, D.; Howell, E. E.; Hirai, J. T.; Warren, M. S. et al. Analysis of hydride transfer and cofactor fluorescence decay in mutants of dihydrofolate reductase: possible evidence for participation of enzyme molecular motions in catalysis. *Biochemistry* **1991**, *30*, 11567−11579.

(21) Birdsall, B.; Bevan, A. W.; Pascual, C.; Roberts, G. C.; Feeney, J. et al. Multinuclear NMR characterization of two coexisting conformational states of the *Lactobacillus casei* dihydrofolate reductase-trimethoprim-NADP+ complex. *Biochemistry* **1984**, *23*, 4733−4742.

(22) Bystroff, C.; Oatley, S. J.; Kraut, J. Crystal structures of *Escherichia coli* dihydrofolate reductase: The NADP+ holoenzyme and the folate-NADP+ ternary complex. Substrate binding and a model for the transition state. *Biochemistry* **1990**, *29*, 3263−3277.

(23) Huang, S.; Appleman, J. R.; Tan, X.; Thompson, P. D.; Blakley, R. L. et al. Role of lysine-54 in determining cofactor specificity and binding in human dihydrofolate reductase. *Biochemistry* **1990**, *29*, 8063−8069.

(24) Baccanari, D. P.; Tansik, R. L.; Joyner, S. S.; Fling, M. E.; Smith, P. L. et al. Characterization of *Candida albicans* dihydrofolate reductase. *J. Biol. Chem.* **1989**, *264*, 1100−1107.

(25) Gangjee, A.; Vidwans, A. P.; Vasudevan, A.; Queener, S. F.; Kisliuk, R. L. et al. Structure-based design and synthesis of lipophilic 2,4-diamino-6-substituted quinazolines and their evaluation as inhibitors of dihydrofolate reductases and potential antitumor agents. *J. Med. Chem.* **1998**, *41*, 3426−3434.

(26) Howard, A. J.; Gilliland, G. L.; Finzel, B. C.; Poulos, T. L.; Ohlendorf, D. H. et al. Use of an imaging proportional counter in macromolecular crystallography. *J. Appl. Crystallogr.* **1987**, *20*, 383−387.

(27) Hendrickson, W. A. Stereochemically restrained refinement of macromolecular structures. *Methods Enzymology*; Academic Press: Orlando, 1985; pp 252−270.

(28) Finzel, B. C. Incorporation of fast Fourier transforms to speed restrained least-squares refinement of proteins. *J. Appl. Crystallogr.* **1987**, *20*, 53−55.

(29) Agarwal, R. C. A new least-squares refinement technique based on the fast Fourier transform algorithm. *Acta Crystallogr.* **1978**, *A34*, 791−809.

(30) Agarwal, R. C. New results on fast Fourier least-squares refinement technique. *Refinement of Protein Structures, Proceedings of the Daresbury Conference*, 1980; pp 24−28.

JM0101444